Supporting Information

On-demand Gelation of Ionic Liquids Using Photoresponsive Organometallic Gelators

Ryo Sumitani,[a] Masamichi Yamanaka [b] and Tomoyuki Mochida *[a,c]

[a]*Department of Chemistry, Graduate School of Science, Kobe University, 1-1 Rokkodai, Nada, Kobe, Hyogo 657-8501, Japan. E-mail: tmochida@platinum.kobe-u.ac.jp*

[b]*Meiji Pharmaceutical University, 2-522-1 Noshio, Kiyose, Tokyo 204–8588, Japan*

[c]*Research Center for Membrane and Film Technology, Kobe University, 1-1 Rokkodai, Nada, Kobe, Hyogo 657-8501, Japan*

Contents

Experimental

Synthesis of [C_6CNEt_3N][Tf_2N]. In a nitrogen atmosphere, an amount of 7-bromoheptanenitrile (1.84 g, 9.7 mmol) was slowly added to a solution of triethylamine (1.0 g, 9.88 mmol) in acetonitrile (2 mL). The solution was subsequently heated at 80 °C for 3 h with constant stirring. The solvent was then removed under reduced pressure. The resultant orange liquid was washed 10 times with hexane and dried under vacuum at 80 °C for 1 h to obtain [C_6CNEt_3N]Br as an orange liquid (2.5 g, 90%). Potassium bis(trifluoromethanesulfonyl)imide (KTf_2N; 6.2 g, 19.4 mmol) was added to an aqueous solution (20 mL) of [C_6CNEt_3N]Br (2.5 g, 8.7 mmol), and the solution was stirred vigorously for 1 h. The resultant [C_6CNEt_3N][Tf_2N] phase was collected and washed three times with water. The orange liquid was dried under vacuum for 3 h at 60 °C. The crude product was purified by column chromatography (alumina, eluent: dichloromethane/acetonitrile, gradient from 1:0 to 0:1). After evaporation of the solvent, the residue was dissolved in acetonitrile and heated to reflux, to which a small amount of activated carbon was added. The activated carbon was then removed by filtration without cooling. After evaporation of the solvent, the residue was dried under vacuum at 130 °C for 6 h. The desired product was a pale-yellow liquid (3.4 g, 69% yield). T_g = −72 °C (DSC). ^{1}H NMR (400 MHz, $CDCl_3$): δ = 1.35 (t, 9H, $N(CH_2CH_3)_3$, J = 7.22 Hz), 1.46 (m, 2H, $NC_3H_6CH_2$), 1.56 (m, 2H, $NC_2H_4CH_2$), 1.70 (m, 4H, $NCH_2CH_2C_2H_4CH_2$), 2.39 (t, 2H, $NC_5H_{10}CH_2$, J = 6.89 Hz), 3.16 (t, 2H, NCH_2, J = 8.51 Hz), 3.29 (q, 6H, $N(CH_2CH_3)_3$). FT-IR (ATR, cm^{-1}): 600, 613, 653, 739, 761, 1052 (S=O), 1134, 1177 (C–F), 1330, 1348, 1397, 1460, 1487, 2246 (CN), 2869 (C–H), 2950 (C–H). Anal. Calcd. for $C_{15}H_{27}F_6N_3O_4S_2$: C, 36.66, H, 5.54, N, 8.55. Found: C, 36.48, H, 5.72, N, 8.38.

Synthesis of [CpRu(L')][$B(CN)_4$] (2-$B(CN)_4$). [CpRu(**L'**)]PF_6 (**2-PF_6**) was synthesized using the procedure identical to that for **1-PF_6** using **L'** (33 mg, 0.083 mmol) and [$CpRu(CH_3CN)_3$]PF_6 (30 mg, 0.069 mmol). The desired product was obtained as an orange viscous liquid (27 mg, 55%). ^{1}H NMR (400 MHz, $CDCl_3$): δ = 0.88 (t, 3H, CH_3, J = 6.89 Hz), 1.26 (m,

18H, $NHC_2H_4C_9H_{18}$), 1.58 (m, 2H, $NHCH_2CH_2$), 3.21 (m, 2H, $NHCH_2$), 4.00 (m, 2H, $PhCH_2$), 5.26 (s, 5H, Cp-*H*), 5.60–5.88 (m, 4H, Ru–Ph–*H*), 6.98 (s, 1H, $NHC_{12}H_{25}$), 7.22 (s, 1H, PhN*H*), 7.10–7.40 (m, 5H, CH_2Ph-*H*). FT-IR (ATR, cm^{-1}): 567 (P–F), 745, 1242, 1289, 1451 (Cp, C=C), 1465, 1482, 1563 (Arene, C=C), 1632 (C=O), 2847, 2916 (C–H). **2-B(CN)$_4$** was synthesized using the procedure identical to that for **1-B(CN)$_4$** using **2-PF$_6$** (21 mg, 0.030 mmol) and $KB(CN)_4$ (14 mg, 0.089 mmol). The desired product was obtained as an orange viscous liquid (13 mg, 65% yield). ^{1}H NMR (400 MHz, $CDCl_3$): δ = 0.88 (t, 3H, CH_3, J = 6.89 Hz), 1.26 (m, 18H, $NHC_2H_4C_9H_{18}$), 1.58 (m, 2H, $NHCH_2CH_2$), 3.21 (m, 2H, $NHCH_2$), 4.00 (m, 2H, $PhCH_2$), 5.26 (s, 5H, Cp-*H*), 5.60–5.88 (m, 4H, Ru–Ph–*H*), 6.98 (s, 1H, $NHC_{12}H_{25}$), 7.22 (s, 1H, PhN*H*), 7.10–7.40 (m, 5H, CH_2Ph-*H*).

Figures and Tables

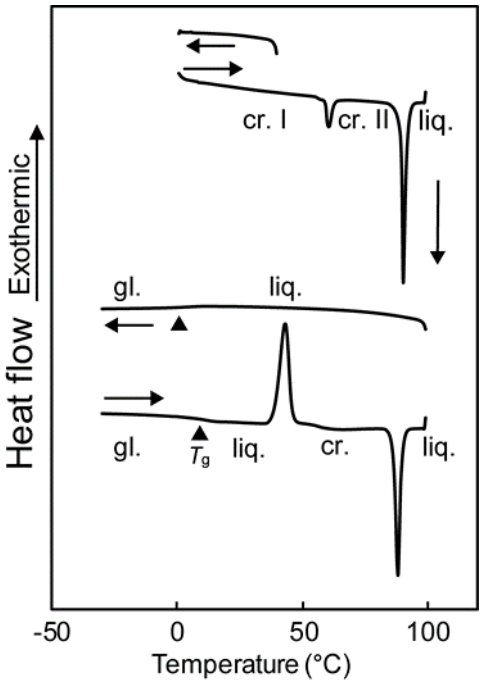

Fig. S1. DSC curve of **1-PF$_6$**, where cr., liq,. and gl. are the crystal, liquid, and glassy states, respectively. A cold-crystallization peak is seen at 45 °C in the second cycle.

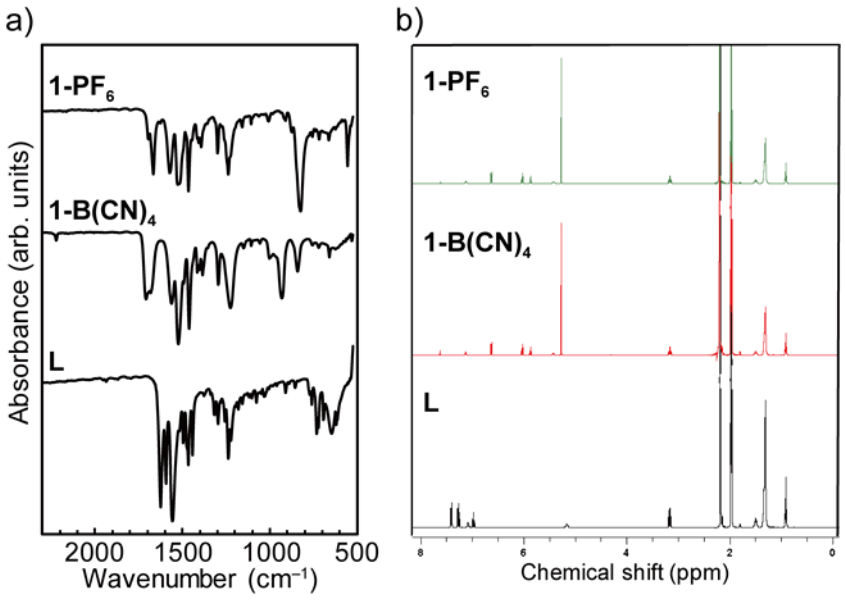

Fig. S2. (a) FT-IR and (b) ^{1}H NMR (CD_3CN) spectra of **1-PF$_6$**, **1-B(CN)$_4$**, and **L**.

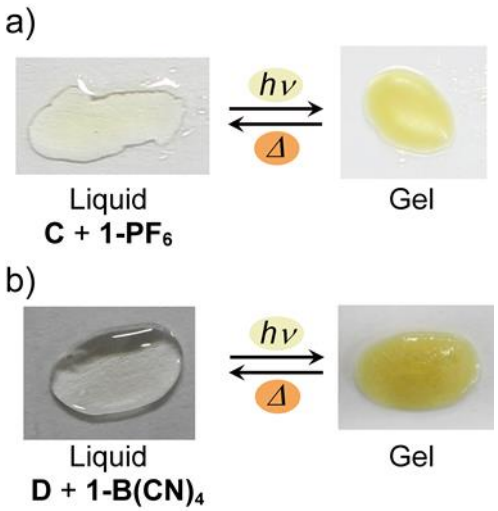

Fig. S3. Photographs of **C** (containing 5 wt.% **1-PF$_6$**) and **D** (containing 5 wt.% **1-B(CN)$_4$**) before and after photoirradiation.

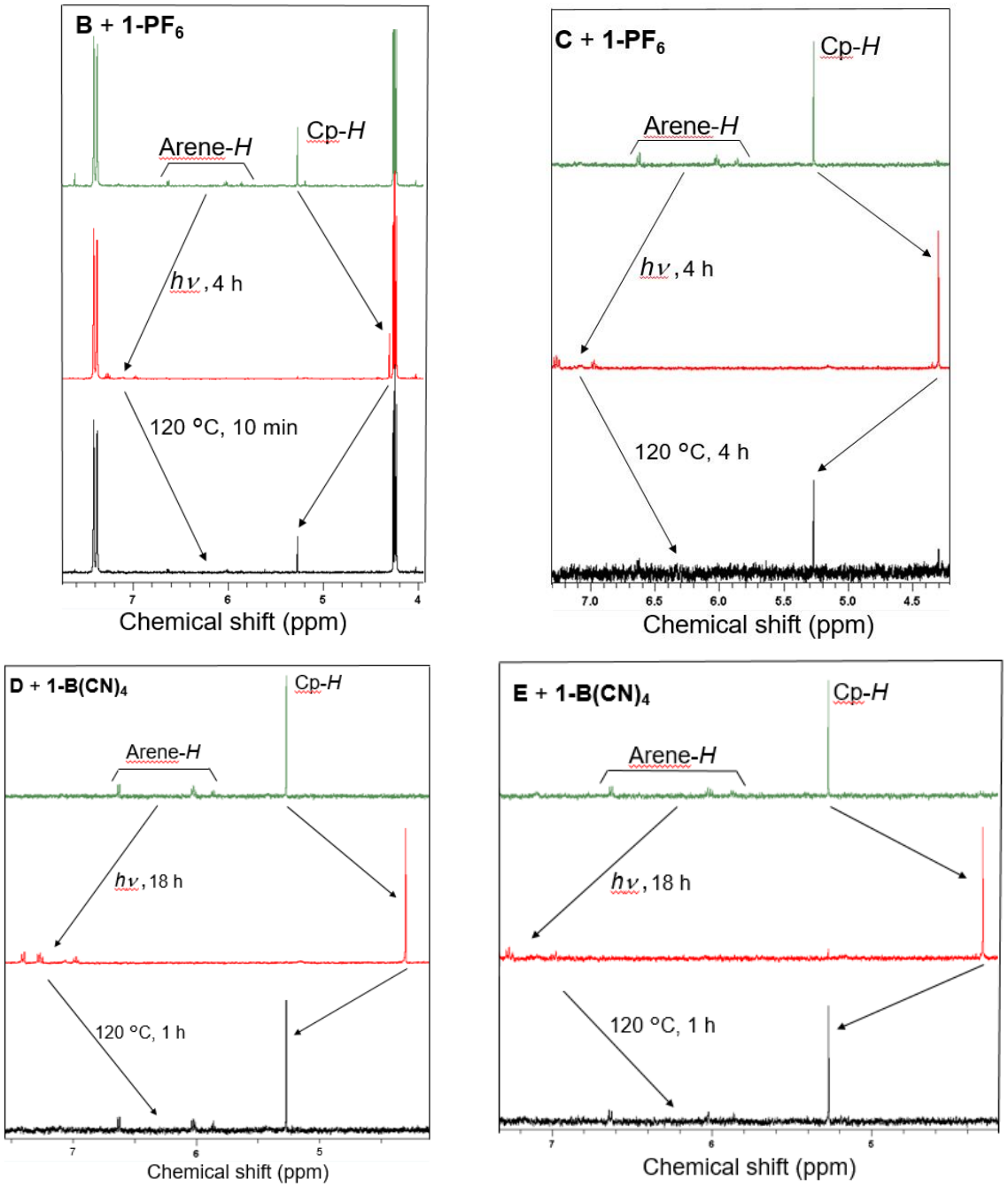

Fig. S4. ^{1}H NMR spectra (CD_3CN) of **B**–**E** (containing 5 wt.% **1-X**) before and after photoirradiation and subsequent heating at 120 °C.

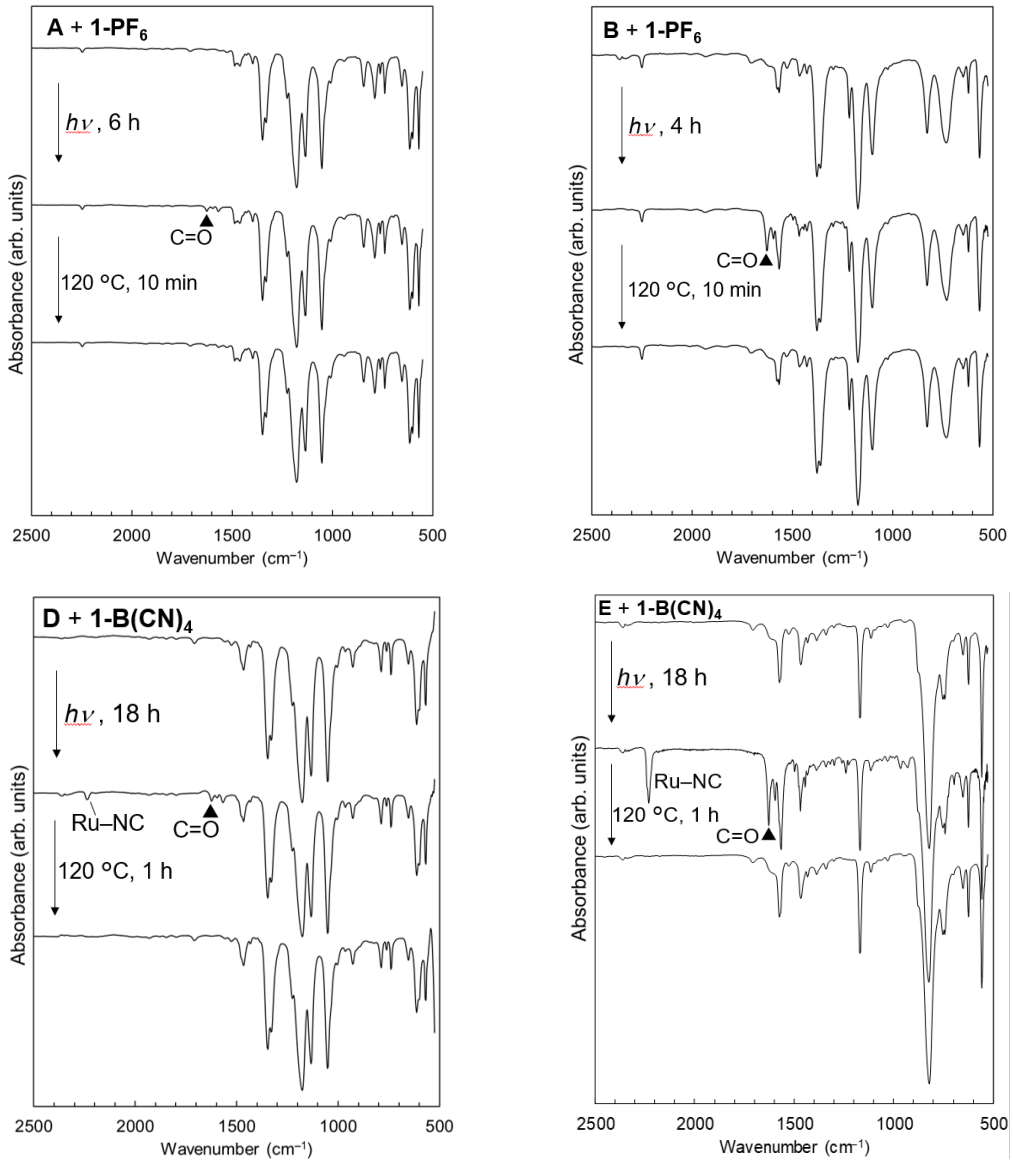

Fig. S5. FT-IR spectra of **A**, **B**, **D**, and **E** (containing 5 wt.% **1-X**) before and after photoirradiation and after subsequent heating at 120 °C.

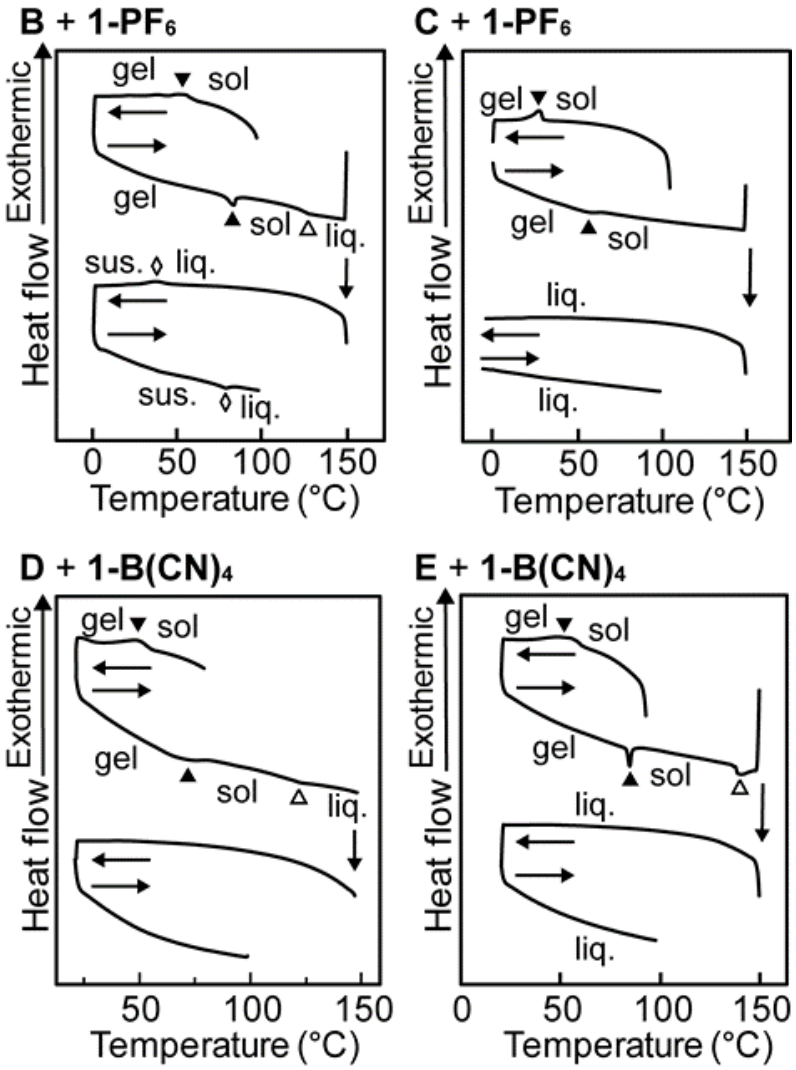

Fig. S6. DSC curves of the ionogels prepared by photoirradiation of **B–E** (containing 5 wt.% **1-X**), where liq. and sus. are the liquid and suspension states, respectively. The peaks corresponding to the gel–sol transition, gelator coordination, and dissolution of the complex are shown by ▲, △, and ◊ symbols, respectively.

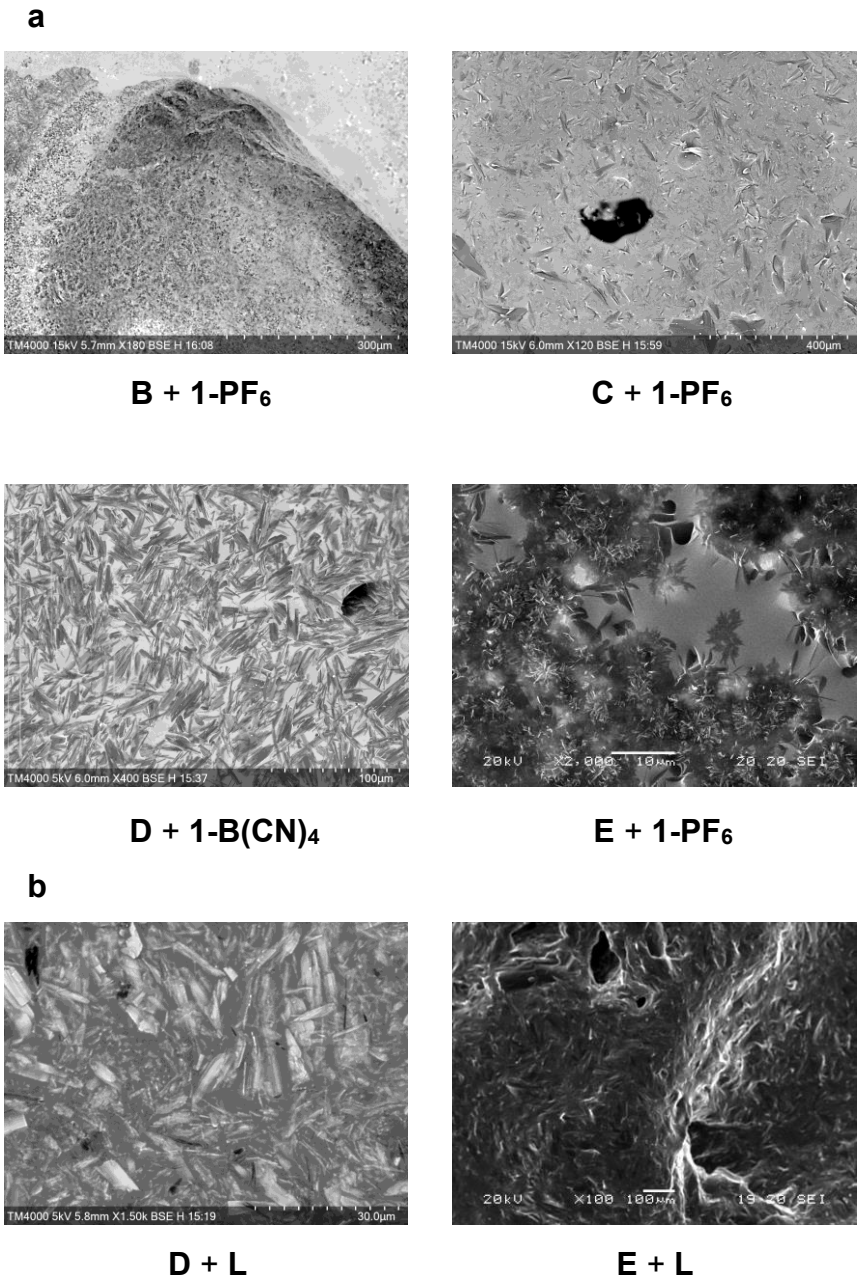

Fig. S7. SEM images of the ionogels prepared by (a) photoirradiation of **B–E** (containing **1-X** 5 wt.%) and (b) addition of gelator **L** (2.4 wt.%) to the ILs. The dark spot in the right figure in (a) is an artifact by electron beam damage.

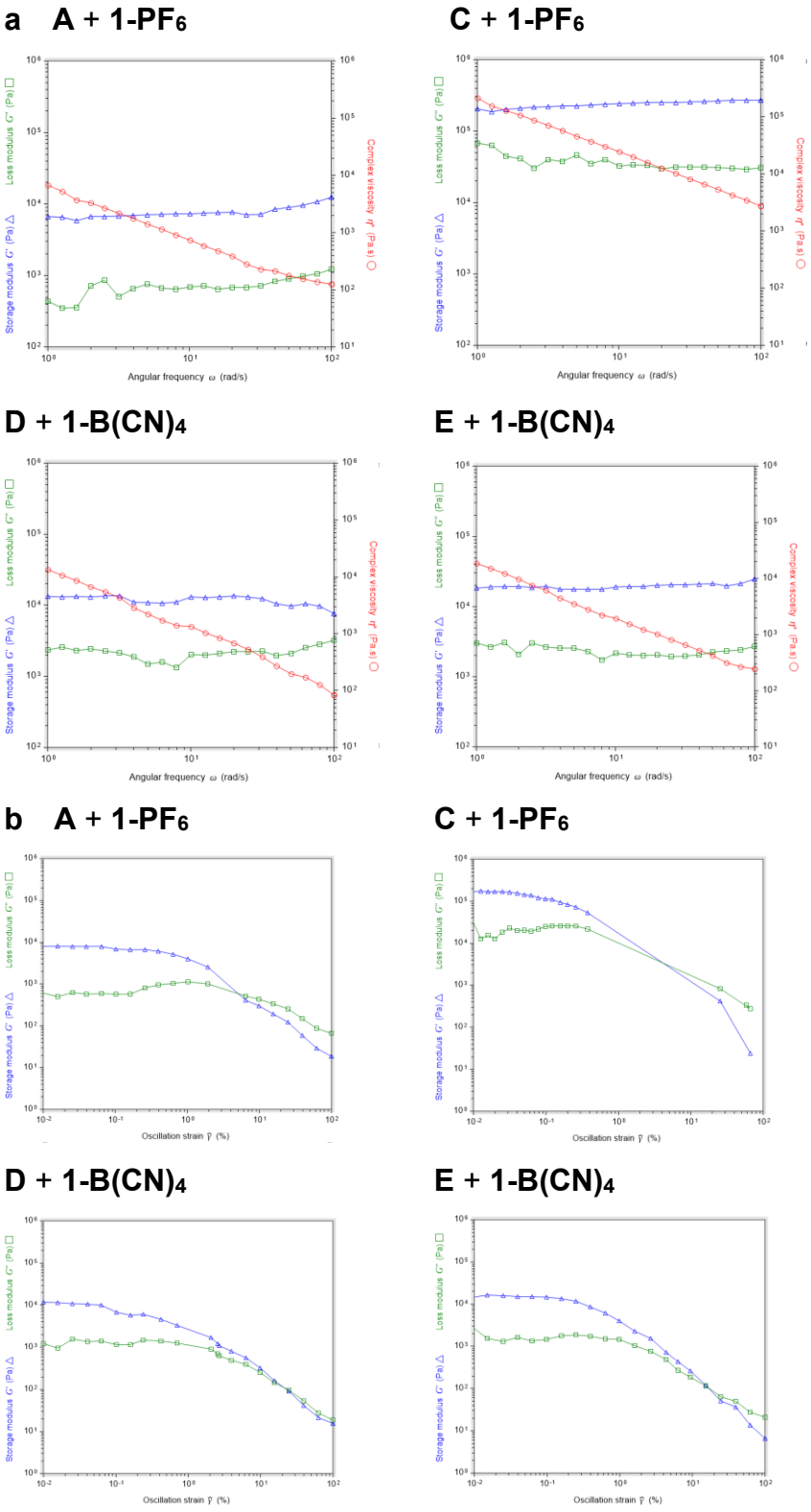

Fig. S8. (a) Angular frequency dependence (25 °C, strain 0.1%) and (b) strain dependence (10 rad s^{-1}) of viscoelastic moduli (G': △, G'': □) and complex viscosity (○) of the ionogels prepared by the photoirradiation of **A**, **B**, **D**, and **E** (containing 5 wt.% **1-X**). Data for **A** and **C** are acquired after thermal treatment (100 °C, 30 s).

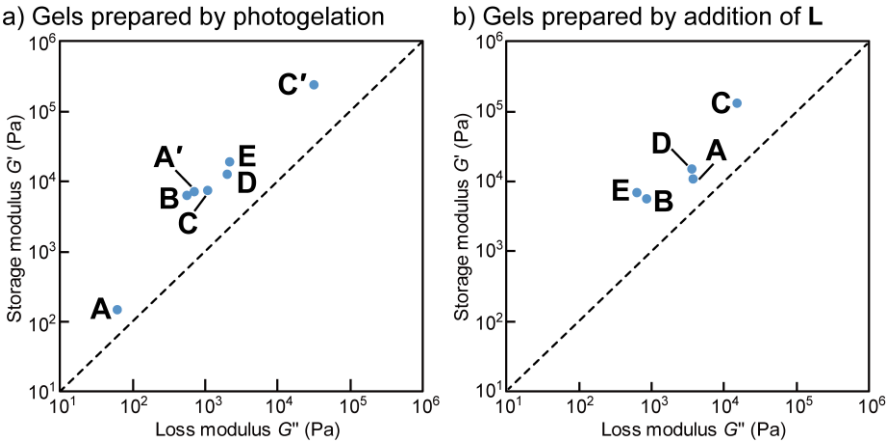

Fig. S9. Plots of storage modulus (G') and loss modulus (G'') of the ionogels prepared by the (a) photoirradiation of **A**–**E** (containing 5 wt.% **1-X**) and (b) addition of gelator **L** (**A**–**C**: 2.4 wt.%, **D** and **E**: 2.5 wt.%) to the ILs. For **A** and **C**, the values after thermal treatment of the gel (100 °C, 30 s) are also plotted (**A′** and **C′**).

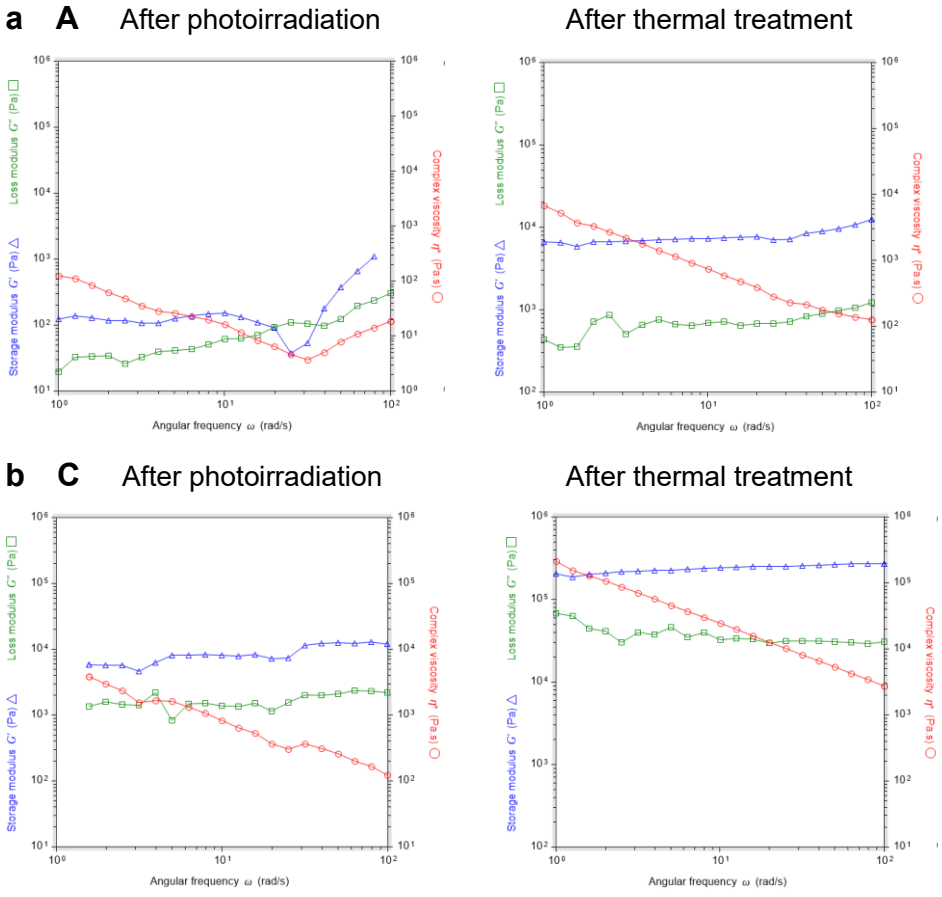

Fig. S10. Angular frequency dependence (25 °C, strain 0.1%) of the viscoelastic moduli (G': △, G'': □) and complex viscosity (○) of gels of (a) **A** and (b) **C** (containing 5 wt.% **1-PF$_6$**) formed upon photoirradiation. Data acquired immediately after photoirradiation (left) and after subsequent thermal treatment (100 °C, 30 s; right) are shown.

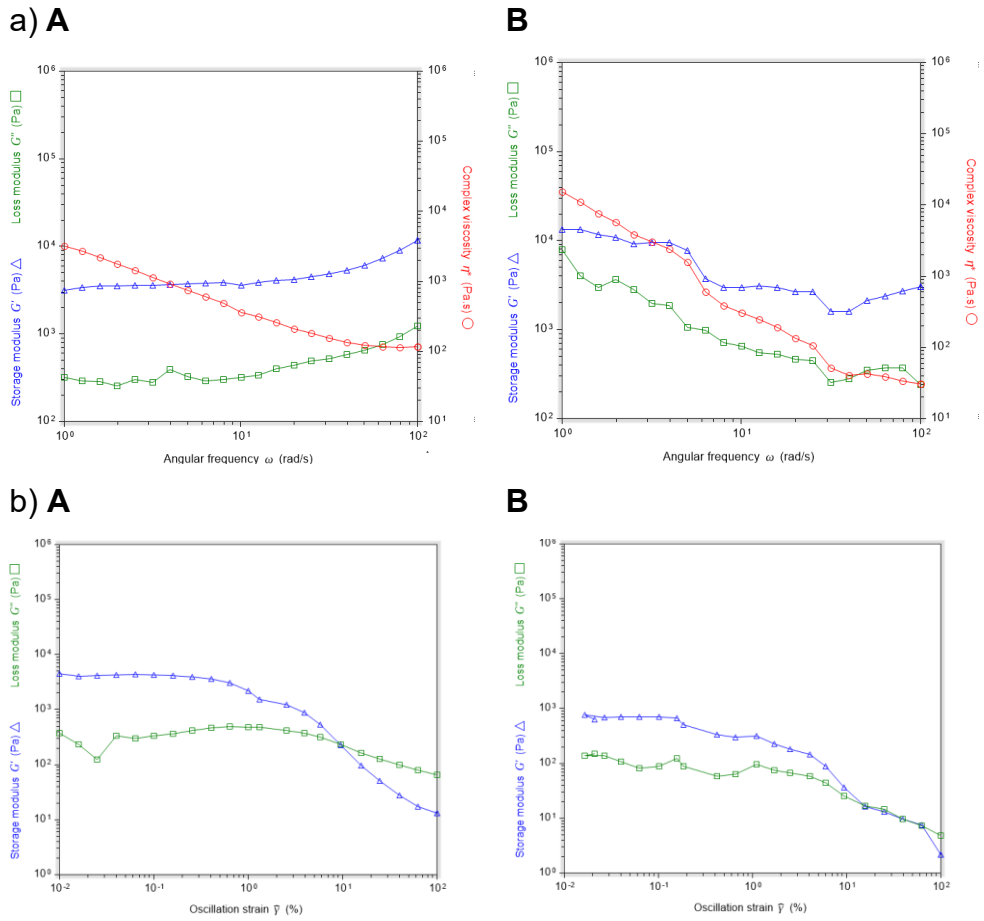

Fig. S11. (a) Angular frequency dependence (25 °C, strain 0.1%) and (b) strain dependence (10 rad s^{-1}) of the viscoelastic moduli (G': △, G'': □) and complex viscosity (○) of ionogels from **A** and **B** (containing 5 wt.% **1-PF$_6$**) after three cycles of photoirradiation. The data for **A** were acquired after thermal treatment (100 °C, 30 s).

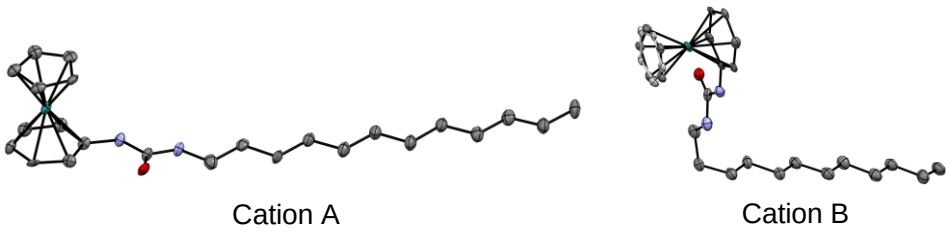

Fig. S12. Molecular structures of the cations of **1-PF$_6$** in the crystal (−183 °C). The disordered moieties of cation **B** are displayed in gray.

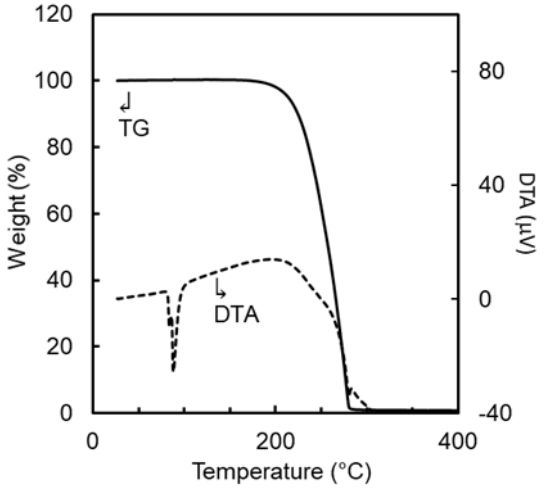

Fig. S13. TG-DTA curves of gelator **L** (10 °C min^{-1}, N_2 atmosphere). There is a melting peak in the DTA curve at around 90 °C.

Table S1. Crystallographic parameters.

	1-PF_6
Empirical formula	$C_{24}H_{37}F_6N_2OPRu$
Formula weight	615.59
Crystal system	triclinic
Space group	$P\bar{1}$
a [Å]	9.637(4)
b [Å]	9.944(5)
c [Å]	27.528(13)
α [°]	95.325(6)
β [°]	97.691(8)
γ [°]	96.476(6)
V [Å^3]	2582(2)
Z	4
ρ_{calcd} [g cm^{-3}]	1.584
μ [mm^{-1}]	0.733
Temperature [K]	90
F(000)	1264
Reflns collected	9148
R (int)	0.0363
Goodness of fit	1.098
$R_1{}^a$, $R_w{}^b$ ($I > 2\sigma$)	0.1041, 0.2448
$R_1{}^a$, $R_w{}^b$ (all data)	0.1393, 0.2643

$^aR_1 = \Sigma||F_o| - |F_c|| / \Sigma|F_o|$. $^bR_w = [\Sigma w (F_o^2 - F_c^2)^2 / \Sigma w (F_o^2)^2]^{1/2}$

Table S2. Gel–sol transition temperature of the ionogels prepared by adding gelator **L**.

IL	T_{gel} (°C)	
	heating	cooling
A[a]	70	41
B[a]	85	57
C[a]	61	33
D[b]	69	45
E[b]	84	47

The amount of gelator added: a) 2.4 wt.% and b) 2.5 wt.%.